V European Conference on Computational Fluid Dynamics
ECCOMAS CFD 2010
J. C. F. Pereira and A. Sequeira (Eds)
Lisbon, Portugal,14-17 June 2010

DETAILED NUMERICAL STUDY OF TURBULENT FLOWS IN AIR CURTAINS

Julian E. Jaramillo[*†], Carles D. Pérez-Segarra[*], Oriol Lehmkuhl[††], Assensi Oliva[*]

[*]Heat and Mass Transfer Technological Centre, Technical University of Catalonia,
C. Colom 11, 08222 Terrassa (Barcelona), Spain
e-mail: cttc@cttc.upc.edu

[†]Institute of Mathematics and Computing Science, University of Groningen
P.O. Box 800, 9700 AV Groningen, The Netherlands
e-mail: julian@cttc.upc.edu

[††]Termo Fluids S.L.
C. Magi Colet 8, 08204 Sabadell, Spain
e-mail: termofluids@yahoo.es

Key words: Computational Fluid Dynamics, Turbulence, Air Curtain, LES, hybrid RANS-LES.

Abstract. *Air curtains are generally a set of vertical or horizontal plane jets used as ambient separator. In order to prevent entrainment, a good air curtain should provide a jet with low turbulence level, and enough momentum to counteract pressure differences across the opening. Consequently, the analysis of the plenum before discharge should be taken into consideration. Hence, the main object of this paper is to study the discharge chamber geometry and the presence of blades for flow orientation at the exit of air curtains. This analysis is carried out in order to understand their influence on the characteristics of the jet produced. Studies presented are based on the detailed numerical simulation of the air curtain discharge plenum by means of Computational Fluid Dynamics method using symmetry-preserving formulation and unstructured meshes. The numerical solutions are compared and the influence of the turbulence model used, boundary conditions and computational domain selected are also investigated. Furthermore, experimental measurements of an air curtain prototype using Hot-Wire Anemometry technique are presented.*

1 INTRODUCTION

An air curtain produces a fan powered air jet used to separate two adjacent spaces at different conditions. As it can be seen in Figure 1, the jet acts as a screen against heat transfer losses/gains, moisture or mass exchanges between these areas. Air curtains are specially appropriate for configurations where effective (solid) barriers become unacceptable for practical, technical or safety reasons[1].

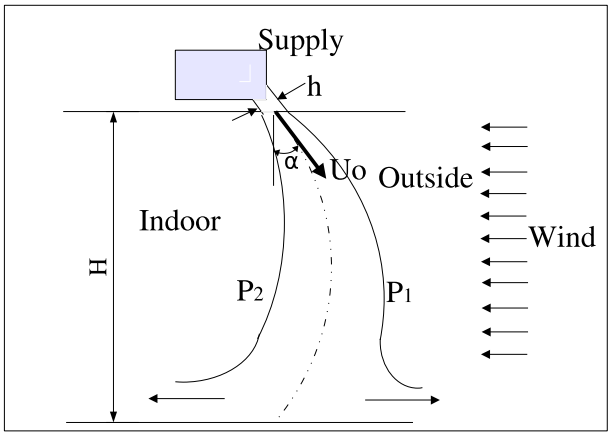

Figure 1: Schematic air curtain representation [1].

Air curtains have been studied analytically, experimentally and numerically. Examples of experimental studies can be found since 60's, when Hetsroni et al.[2] studied air entrainment-spill mechanism across air curtains. Works by Hayes and Stoecker[3], Howell and Shiabata[4], Faramarzi and Kemp[5], Guyonnaud et al.[6], Havet et al.[7], and Chen and Yuan[8] are some other experimental works that can be mentioned. Analytical studies have been carried out by Partyka[9], and Sirén[10]. Furthermore, numerical studies of air curtains using computational fluid dynamics (CFD) are also found in the literature. For example, Stribling et al.[11], Ge and Tassou[12], and Navaz et al.[13] presented a computational study of an air curtain in a vertical display cabinet. Whereas, Cui and Wang[14] used CFD method to evaluate the energy performance of air curtains in horizontal refrigerated display cabinets. Moreover, combinations of CFD and experimental works have been presented by Navaz et al.[15] and Foster et al.[16]. Recently, various works dealing with air curtains placed in door openings to separate two different ambients have been published. Costa et al.[17] restricted the study to a two dimensional situation taking into account stack effect, and analysed the influence of the height of the curtain, discharge angle and velocity, on the sealing efficiency of an air curtain. Foster et al.[18, 19], and Jaramillo et al.[20] evaluated the effectiveness and three dimensional effects of air curtains in the entrance of refrigerated rooms. Finally, Navaz et al.[21] have addressed, numerically and experimentally, the effects of the velocity profile at the discharge air grill on the amount of entrained air into an open refrigerated display case. As it can be seen only the last work considered the effect of the

air velocity distribution before air curtain discharge nozzle. Furthermore, that study was centred on display cabinets.

In the technical dimensioning of an air curtain both a fluid-dynamic approach and a thermal approach are needed. In the first case it is necessary to determine the pressure differences across the opening ($P_2 - P_1$) in a given set of weather conditions, in order to fix the required nozzle width (h), jet velocity exit (Uo) and discharge angle (α) (see Figure 1). In the thermal dimensioning is important to establish energy losses. The heat flux through the opening with the air curtain system is due to the jet turbulence level and the net mass flow across it. Owing to the fact that air is entrained into the jet from both sides, in part because of mixing process and part when the jet hits the floor, the air curtain cannot totally prevent heat and/or mass transport across the doorway, but remarkably reduce them.

In order to prevent entrainment, an air curtain should provide a jet with low turbulence level, enough momentum to counteract pressure differences across the opening ($P_2 - P_1$) due to wind, buoyancy and the pressure difference due to imbalance of ventilation system across it[21], and in most of the cases a discharge parabolic profile skewed to the protected zone. Consequently, the analysis of the plenum before discharge should be taken into account.

The main objective of this paper is to carry out a detailed study of the discharge plenum of an air curtain intended to be placed on a doorway and the influence of blades for flow orientation, on the discharge jet produced by the air curtain. Advanced computational fluids dynamics techniques are used. Moreover, experimental measurements are carried out in order to determine the actual fluid flow characteristics of an air curtain prototype.

Most of the air curtains produce discharge jets in turbulent regime. As it is well known, turbulent flows are three-dimensional, unsteady, and present a wide range of scales of motion and time. Therefore, direct numerical simulations of the Navier-Stokes equations (DNS) is generally restricted to simple geometries or low Reynolds numbers. Then, in this work a statistical technique based on volume filtering known as large eddy simulation (LES) is used. In LES, the smallest scales, the subgrid-scale eddies, are modelled but the larger ones, which are directly affected by boundary conditions and geometry, are solved in detail (three-dimensional and unsteady). The smallest scales are nearly isotropic and have, to some extent, universal characteristics. Thereby, they can be represented by relatively simple models[22]. However, there is still required a fine grid in the near wall region, what has severely slowed the development of LES for flows of practical interest. Then, models involving a combination of LES and Reynolds Navier-Stokes Simulation (RANS) can be an interesting option that is also explored in this work. In these kind of models the great computational cost of solving the small-scale motions near the walls is avoided[23].

The numerical methodology applied in the present paper is based on volume finite techniques. Governing partial differential equations are converted into algebraic ones using unstructured meshes. The system of equations is solved with full parallel direct sparse linear solvers by means of a full parallel three-dimensional CFD code. Second-order schemes are used for transient and spatial discretization. Local grid refinement is used[24]. Furthermore, the mathematical formulation used in this work is based on symmetry-preserving discretization of the governing equations, which assures that some important properties of the Navier-Stokes equations are retained in the discretization process[25].

In the first part of this work the actual velocity profile produced by an air curtain prototype is determined by using hot wire constant temperature anemometry technique (CTA)[26]. Then, experimental results are used to extract inlet boundary conditions for CFD simulations. After verification of the numerical solutions, parametric studies are carried out in an effort to identify the influence of blades for flow orientation placed at the air curtain discharge.

2 GOVERNING EQUATIONS

The governing equations assuming incompressible Newtonian fluid with constant thermophysical properties, and non-participant radiant medium, can be written as follows

$$\vec{\bigtriangledown} \cdot \vec{v} = 0 \tag{1}$$

$$\frac{\partial \vec{v}}{\partial t} = -(\vec{v} \cdot \vec{\bigtriangledown})\vec{v} + \nu \bigtriangledown^2 \vec{v} - \frac{1}{\rho} \bigtriangledown p \tag{2}$$

$$\frac{\partial T}{\partial t} = -(\vec{v} \cdot \vec{\bigtriangledown})T + \alpha \bigtriangledown^2 T \tag{3}$$

where, ν is the kinematic viscosity and α is the thermal diffusivity. In case of isothermal conditions, the energy equation (3) is not needed.

3 ACTUAL FLUID FLOW CHARACTERISTICS

In this section illustrative results of the experimental work carried out in order to characterise the air curtain fluid-dynamic field are presented. Hot wire constant temperature anemometry (CTA) is used to measure velocity.

3.1 Experimental Setup

The air curtain is placed vertically in a space with enough room to avoid any interference with surrounding walls. Discharge velocity profiles at various locations downstream air curtain discharge nozzle, and fans outlet inside the plenum chamber are studied. Hence, a positioning device that allows horizontal and vertical displacements is needed. The horizontal movement is accomplished by using an automatic system type cantilever

with stationary steeping motors and mobile axis body. The vertical positioning is done by means of a portal axis toothed belt driven linear system. The movement is controlled remotely by means of RS-232 ports. With this system a positioning accuracy of $\pm 1mm$ can be achieved.
Constant temperature hot wire anemometry (CTA) is used for velocity measurements. Thermal anemometry measures fluid velocity by sensing the changes in heat transfer from a small, electrically heated element exposed to the fluid. In CTA method, the cooling effect produced by the flow passing over the sensor is balanced by the electrical current given to the sensor. The change in current due to a change in flow velocity shows up as a voltage at the anemometer output. Finally, the anemometer is linked to a personal computer, where data are analysed. The parameters defining the data acquisition in CTA are the sampling rate and the number of samples. Their values depend primarily on the specific experiment, the required data analysis and the acceptable level of uncertainty. Time-averaged analysis requires non-correlated samples, which can be achieved when the time between samples is at least two times larger than the integral time scale of the velocity fluctuations. The number of samples depends on the desired uncertainty and confidence level of the results[26].

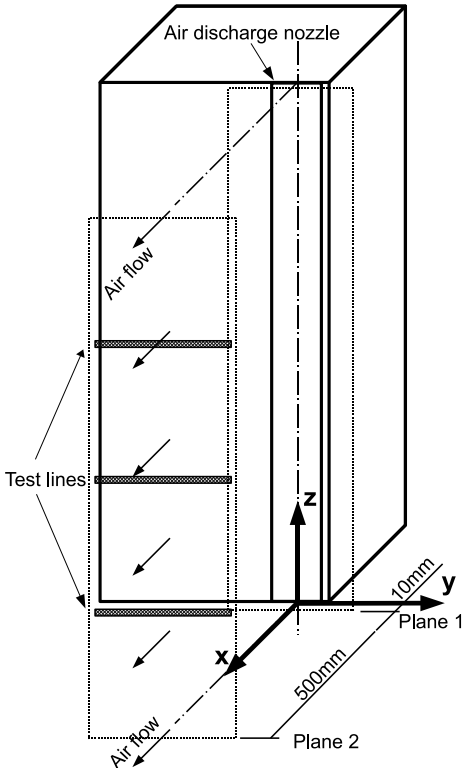

Figure 2: Measurements location and assumed coordinate system.

In this work TSI-IFA300 CTA unit, and TSI 1241-20 and 1210-20 sensors are used. Sensor calibration is carried out by means of an automated calibrator TSI-1129 model. In general, a sampling rate of 200 Hz and a sampling time of 20 s in each measured point are selected. Data obtained for each one of the velocity components measured are:

- Mean velocity: $U_{mean} = \frac{1}{N}\sum_{i=1}^{N} U_i$
- Standard deviation (root mean square): $U_{rms} = \sqrt{\frac{1}{N-1}\sum_{1}^{N}(U_i - U_{mean})^2}$
- Turbulent stress: $\overline{u'u'} = (U_{rms})^2$
- Turbulence intensity: $T_u = I = U_{rms}/U_{mean}$

3.2 Illustrative Experimental Data

A schematic representation of locations where measurements are done and reference system used is presented in Figure 2. Furthermore, experimental data are acquired inside the discharge plenum, at the fans discharge to investigate its relation with the jet produced by the air curtain, and to obtain inlet values for the CFD simulations. $Plane\_1$ and $\_2$ in Figure 2 indicate location of measurements to establish the discharge jet velocity characteristics of the prototype studied. The first one ($Plane\_1$) is located near discharge nozzle, at 10 mm in x-direction. $Plane\_2$ is placed downstream at $x = 500$ mm. In $Plane\_1$ measurements are done each 10 mm in y-direction, and each 20 mm in z-direction. While in $Plane\_2$, measurements are acquired at three test lines $z = 250,\ 500$ and 750 mm.

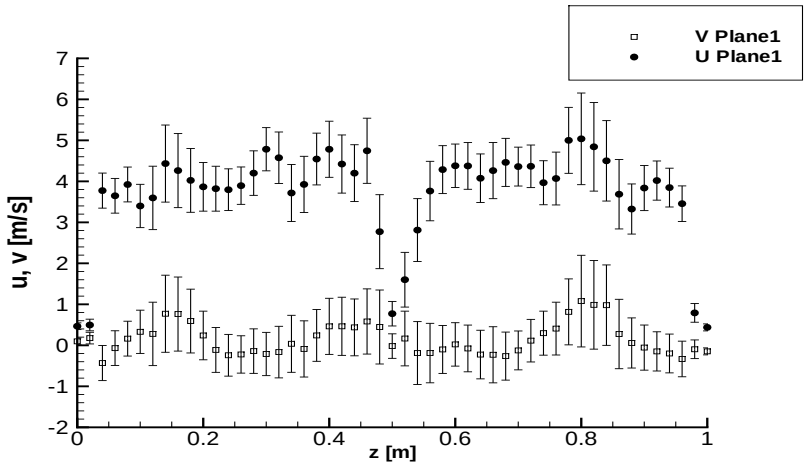

Figure 3: Air curtain discharge velocity profile. $Plane\_1$ ($x = 10$ mm, $y = 0$ mm).

From the experimental data obtained at the fans outlet (not shown), it is observed as the measured profile exhibits two minimums, being the lowest the one near the upper part of each one of the fans. Therefore, produced velocity profile is highly irregular. Regarding fluctuating velocities, the fans produce turbulence intensities between 10% and 40%. These data reflect the relevance of the air curtain plenum in order to have a more homogeneous velocity profile at the discharge nozzle.

3.2.1 Air Curtain Flow Characterisation Near Discharge Nozzle, $x = 10\ mm$

Once fans have been studied, the attention is focused on the air curtain discharge. Results of the experiments carried out with a TSI1241-20 probe are plotted in Figures 3 and 4 for $Plane\_1$. In these figures is observable the irregularity of the discharge velocity profile. This roughness contributes to increase eddies formation and thereby turbulence increasing.

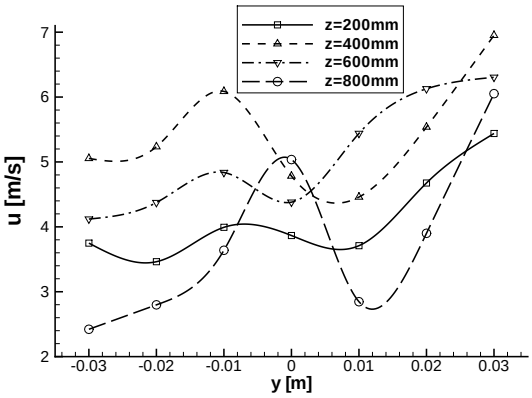

Figure 4: Transverse profiles of discharge velocity. $Plane\_1$ ($x = 10\ mm$) at four z-positions.

Reviewing streamwise velocity u-component (x-direction), in Figure 3 it is possible to distinguish three regions with lower velocity: near the bottom, central and top region ($z = 0$, $z = 500$ and $z = 1000\ mm$). Top and bottom minimums are due to the presence of air curtain wall edges. Whereas, the minimum in the centre corresponds to the device used to mount the blade for flow orientation. Even though, a different profile is observed at each z-location, it can be seen in Figure 4 that regions with the highest u-velocity values are near the external border of the curtain ($y = 30\ mm$). Furthermore, at the four locations shown a secondary velocity maximum is observed near the interior side of the blade for flow orientation.

Turning to normal velocity (y-direction) component, it can be seen in Figure 3 that it presents values up to 1 m/s, which are lower than the ones measured for the u-velocity

component. Spanwise velocity component is neglected. Therefore, if discharge angle is set to zero, air curtain discharge velocity can be considered one-dimensional, flowing in x-direction.

Regarding turbulence level, bars appearing in Figure 3 indicate standard deviation of velocity, what in turbulent flows represents the fluctuating part of the velocity or root mean square velocity (u_{rms} or v_{rms}). These fluctuating velocities produce turbulence intensities between 10% and 40% for the U-velocity component and much higher for V-velocity component. However, measurements using HWA must be taken with care in regions where the mean velocity is around zero[26].

Finally it is worth to note that a correspondence is observed in the irregularities between both fans outlet and discharge nozzle velocity profiles. Therefore, it is necessary to improve fans discharge homogeneity or to place some homogeniser in the plenum chamber to obtain a more uniform velocity profile at the air curtain discharge nozzle.

3.2.2 Jet Produced Downstream Air Curtain Discharge Nozzle, $x = 500\ mm$

In Figure 5, experimental data acquired at *Plane_2* ($x = 500\ mm$), and at three spanwise test lines ($z = 250,\ 500$ and $750\ mm$) are plotted.

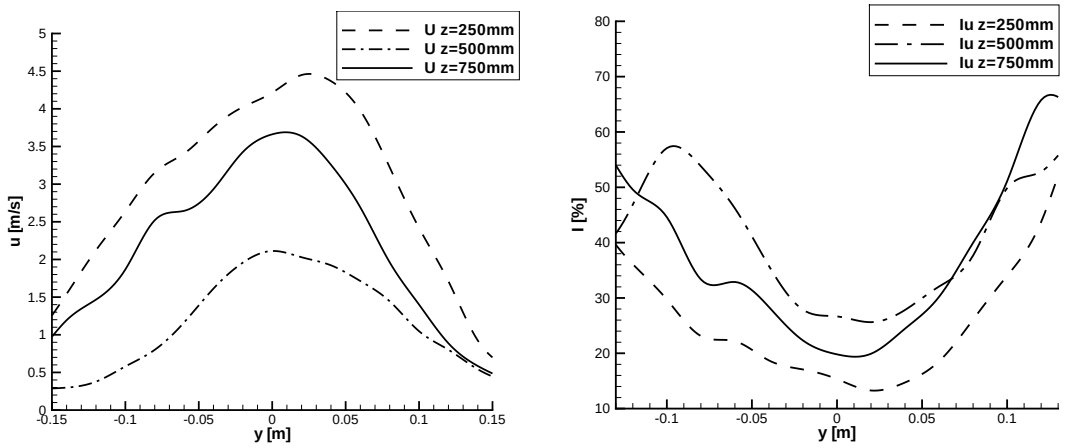

(a) Mean velocity (b) Turbulence intensity

Figure 5: Streamwise experimental data at *Plane_2* ($x = 500\ mm$).

As it can be observed in this Figure, the jet maximum presents a displacement towards the external part of the air curtain ($y = 50\ mm$). Furthermore, the asymmetry in z-direction observed near the discharge nozzle is still encountered at this location downstream. It is also remarkable the reduction of the jet velocity in the central line as

consequence of the device used to mount the blade for flow orientation present in the air curtain prototype studied (see Figure 5(a)). Moreover, turbulence intensity remains high near jet centreline, and as expected, increases towards the jet borders. Reduction observed in the internal border ($-10\ mm < y < -15\ mm$) in the central test line ($z = 500\ mm$) is not credible because it responds to the low mean velocity measured in that region, where buoyancy effect can influence HWA sensor behaviour[26].

In the next experiment, the blade used to orient the air curtain discharge is oriented 15^o towards the external part of the air curtain ($y-$positive) to study its ability to change jet flow. Results obtained at $x = 500\ mm$ ($Plane\_2$), and $z = 250,\ 500$ and $750\ mm$ are shown in Figure 6. In this Figure it is possible to observe as the highest values for the streamwise velocity are measured in the test line corresponding to $z = 250\ mm$. The lowest turbulence level is also seen in this line.

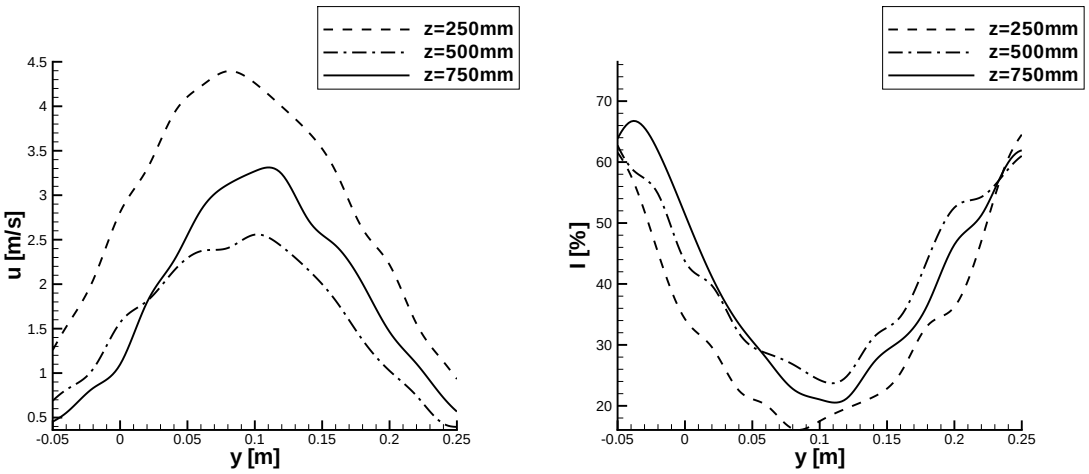

(a) Mean velocity (b) turbulence intensity

Figure 6: Streamwise experimental data at $Plane\_2$ ($x = 500\ mm$) when blade angle is set to 15^o.

The maximum velocity for a discharge angle of 15^o at this x distance should be located around $y = 135\ mm$, however as shown in Figure 6(a) the peak at the three test lines studied is placed approximately at $y = 100\ mm$. This indicates that the blade used to orient the flow is not enough to modify the jet flow direction. This behaviour is also observed in the numerical results presented in the following section. Furthermore, reviewing turbulence intensities in Figure 6(b), similar values for a discharge angle of 15^o to those without setting an angle ($\alpha = 0^o$) can be observed. Moreover, minimum turbulence values coincide with the location of the maximum velocities.

4 NUMERICAL METHODOLOGY

A new general purpose CFD code, called TermoFluids[24], is used in this work. The code uses efficient algorithms, which work adequately on slow networks of personal computers clusters. Governing partial differential equations are converted into algebraic ones using unstructured collocated meshes, and symmetry-preserving discretization, which preserves the purely redistributive character of the convection term[25]. Pressure-velocity coupling is solved by means of fully explicit fractional step algorithm. For temporal discretization, a central difference scheme is used for transient term, an implicit first-order Euler scheme is employed for the pressure gradient term and continuity equation, whereas a second-order Adams-Bashforth scheme is applied for convection, diffusion and buoyancy terms. Conservative spectrum-consistent second order schemes, which preserve kinetic energy even in coarse meshes, are applied for the spatial discretization[25]. Local refinement of the grid, where large velocity gradients exist, is applied. Partitioning of the computational domain is carried out by means of MeTIS software.

For the solution of the pressure (Poisson) equation, a direct Schur-Fourier decomposition is used. Taking into account the periodicity of the domain in the homogeneous direction, a Fourier diagonalisation is applied. It decomposes the 3D problem into a set of 2D independent ones, which are solved using a parallel Schur decomposition[27].

5 NUMERICAL STUDIES

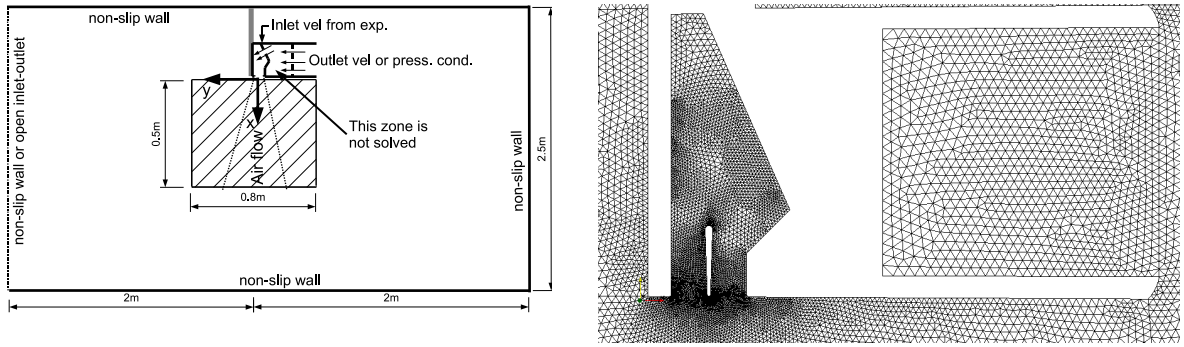

(a) Domain (b) Grid example

Figure 7: Computational details.

Due to the shortcomings of numerical simulations using traditional RANS models, turbulent behaviour of the flow can be better solved by means of LES modelling. In Large Eddy Simulation (LES), the large three-dimensional unsteady turbulent motions are directly represented, whereas the effects of the smallest scales of motion are modelled. The application and validity of this approach is supported by the observed similarity of the

small scales[22]. In this work a LES modified dynamic subgrid-scale model[28] applying a least squares approach to minimise errors proposed by Lilly[29], adapted to unstructured meshes[30] (hereafter referred as LES-DEV) is used. However, as it was commented before, due to LES grid requirements near solid walls, it still demands considerable computational resources. This limitation can be avoided if hybrid LES/RANS models are used. The main idea of these models is to modelise the wall layer with a RANS model, while the external zone is solved with LES. Therefore, an hybrid RANS/LES model[23] (hereafter referred as DES) is selected for comparison purposes. Furthermore, coarse DNS simulations obtained without any model, but using the formulation based on symmetry-preserving discretization (referred as cDNS) are considered.

This section is focussed on the detailed numerical study of air curtain discharge plenum. The influence of the blades placed at the discharge nozzle for flow orientation on the jet produced by the air curtain is also analysed. In Figure 7, a sketch of the computational domain used in the numerical studies carried out is shown. The air movement before fans inside air curtain is not simulated, but the experimental data obtained at the discharge of the fans is used to obtain a mean velocity to feed air flow inlet boundary conditions in the numerical simulations. The configuration studied in this work is considered isothermal. Geometry selected is similar to the one used in the experiments for comparison purposes. Hence, a velocity of approximately 4.5 m/s is imposed. Firstly, it is fixed with an inlet angle respect to the inlet opening according to the experimental data (referred as u_{in}^{α}). Then, to study the influence of inlet angle, the velocity is set normal to the inlet opening (u_{in}). Furthemore, two computational domains have been considered. A small one taking into account only part of the discharge jet downstream until $x = 0.5\ m$ for $-0.4\ m \leq y \leq 0.4\ m$ (dashed region in Figure 7, referred as DomainS), and a larger studying two rooms of $2\ m \times 2.5\ m$ at each side of the air curtain discharge nozzle (referred as DomainL). Moreover, two possibilities are considered for the boundary condition at the left of the domain. It can be a wall with non-slip conditions or it can be an open inlet/outlet boundary. Therefore, according to the left boundary, at the suction of the air curtain a pressure outlet boundary condition or a given velocity that satisfies mass conservation inside air curtain is prescribed, respectively. At the top and bottom planes, a periodic boundary condition is imposed. The other boundaries are walls with non-slip conditions.

An example of the grid used near air curtain unit is shown in Figure 7(b). A plane of the grid is formed by approximately 75000 control volumes. The grid is refined near the blade for flow orientation, and to a less extent, inside air curtain plenum and downstream discharge nozzle. In Figure 8, an example of the mean velocity magnitude distribution is shown using $DomainL$, LES-DEV model and u_{in}^{α}. The blade is oriented vertically and the discharged jet should flow vertically in $x-$direction. As it can be observed in this Figure, there are two recirculation inside the air curtain plenum. The bigger one is placed in the

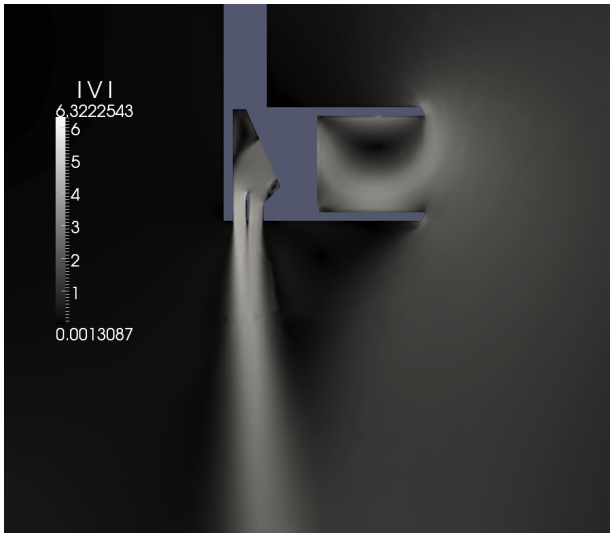

Figure 8: Example of predicted magnitude velocity contours.

upper part of the plenum. The second one, which is smaller, is in the right side, near to the inlet. Moreover, a region of underpressure below air curtain device is seen, where an almost stagnation region is present.

5.1 Verification and Validation of Numerical Results

Mean quantities presented are averaged in time and in the spanwise direction. The evolution of instantaneous variables in three points of the domain as function of time is plotted in Figure 9(a). Taking into account results shown for the points studied, the time integration is started after $600to$, and mean variables are averaged over a time interval of $400to$. Where a time unit (to) is obtained dividing opening section (length) by u_{in}. Moreover, similar results are found when the number of planes in spanwise direction is increased from 8 to 16. Therefore in the parametric study presented below 8 planes are used in the numerical simulations.

The influence of having a wall at the left side of the computational domain has been studied. When the left boundary is open, an overpressure is generated in the right side room. As a result of this, the discharge jet produced by the air curtain is slightly displaced towards the left side. Therefore, a wall is placed in this boundary in order to avoid this effect.

To validating numerical results, they are compared with our own experimental data presented in section 3. Results for the streamwise mean velocity profiles at $Plane\_2$ ($x = 500\ mm$) using $DomainL$, u_{in}^{α}, and LES-DEV model, are shown in Figure 9(b). Comparison with experiments reveals some differences. These discrepancies can be mainly attributed to the periodic hypothesis used in the simulation in the spanwise direction.

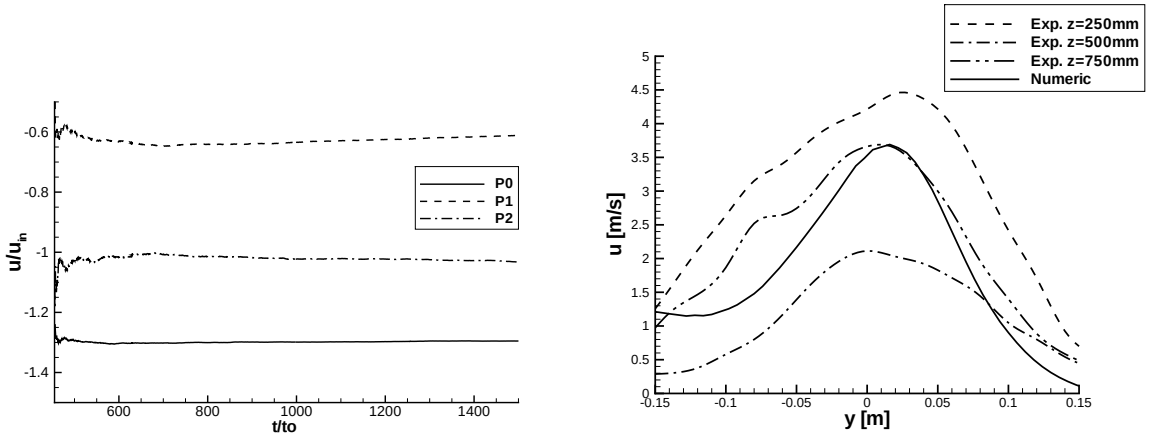

(a) (b)

Figure 9: Left: time evolution of mean dimensionless streamwise velocity at three different points. $P0: x = 0\ mm,\ y = 15\ mm$; $P1: x = 0\ mm,\ y = 0\ mm$, and $P2: x = 100\ mm,\ y = 0\ mm$. Right: validation numerical results at $Plane\_2$ ($x = 500\ mm$).

Therefore, if a more accurate solution is desired, the simulation should be carried out considering the discharge plenum using fully three-dimensional geometry. However, as it can be seen, there is an overall agreement between predicted numerical results and experimental data.

5.2 Illustrative Numerical Studies

The influence of inlet boundary conditions, computational domain and turbulence model is now analysed. Inlet conditions are set by imposing a mean velocity with a given angle, and with or without superimposed fluctuations. These fluctuations are introduced to simulate the turbulence level by means of a Gaussian density function varying around a fixed turbulence intensity of 15%[31]. The mean velocity profiles obtained at the discharge nozzle, using cDNS, $DomainL$ and u^{α}_{in}, with and without turbulence intensity are comparable. However, due to the fact that a turbulence level of the order of 15% has been measured, it is imposed in all the studies carried out hereafter. Furthermore, to establishing the influence of the inlet velocity angle on the discharge jet produced, an inlet velocity normal to the inlet opening is now imposed (u_{in}), using $DomainL$ and LES-DEV model. Streamwise velocity profiles at $Plane\_2$, are plotted with solid line for u^{α}_{in} and u_{in} in Figures 9(b) and 11(b), respectively. Since the amount of mass effectively entering the domain when u_{in} is imposed a higher velocity is predicted, but the jet direction is nearly the same. So then, air curtain fans should be placed in such a way that they generate a velocity normal to the plenum inlet opening.

It is also important to compare results obtained if different turbulence models are used. Therefore, the two models mentioned at the beginning of this section,i.e. LES-DEV

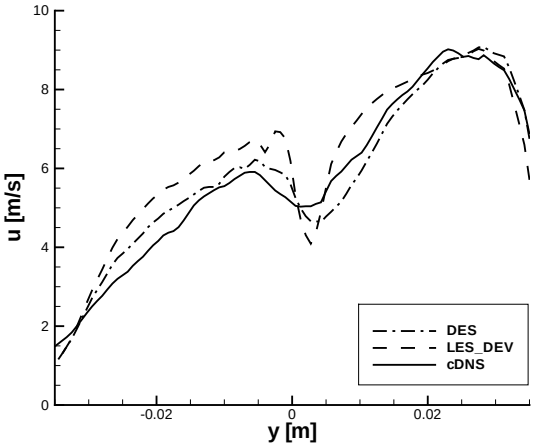

Figure 10: Turbulence model comparison at $Plane\_1$ ($x = 10\ mm$) using $DomainS$.

model [30] and DES model[23], are here analysed. Furthermore, a coarse DNS simulation (cDNS) is performed for comparison purposes. In an attempt to reduce computational effort, the size of computational domain downstream air curtain discharge nozzle used in these studies is reduced to $DomainS$. However, as it will be explained later numerical results are affected by this change. Predicted mean streamwise velocity profiles at $Plane\_1$ ($x = 10\ mm$) are plotted in Figure 10. As it can be seen, similar results are obtained for the three simulations. Nevertheless, LES-DEV model presents a more marked depression in the velocity profile in the near wake downstream the trailing edge of the blade for flow orientation. Furthermore, the three formulations predict a maximum near the front (exterior) discharge plenum wall.

Attention is now focussed on the effect of the size of the computational domain downstream of the air curtain discharge nozzle. Results using LES-DEV model and u_{in} are shown in Figures 10 and 11(a), for $DomainS$ and $DomainL$, respectively. Because of the reduction in the computational domain size, an incorrect increase in the streamwise velocity distribution near the external air curtain discharge plenum wall is observed in Figure 10.

The discharge jet produced when using one or two blades for flow orientation, and their efficiency to change the jet direction are analysed in this section using LES-DEV model, $DomainL$ and u_{in}. Firstly attention is focussed on the use of a single blade. Three angles are studied for this configuration. Hence, the angle is set to 0^o, 15^o and -15^o. Where a positive angle means it is oriented towards the positive y-direction (left side Figure 7(a)).

In Figure 11(a) results at the discharge nozzle section ($Plane\_1$) are shown. A depres-

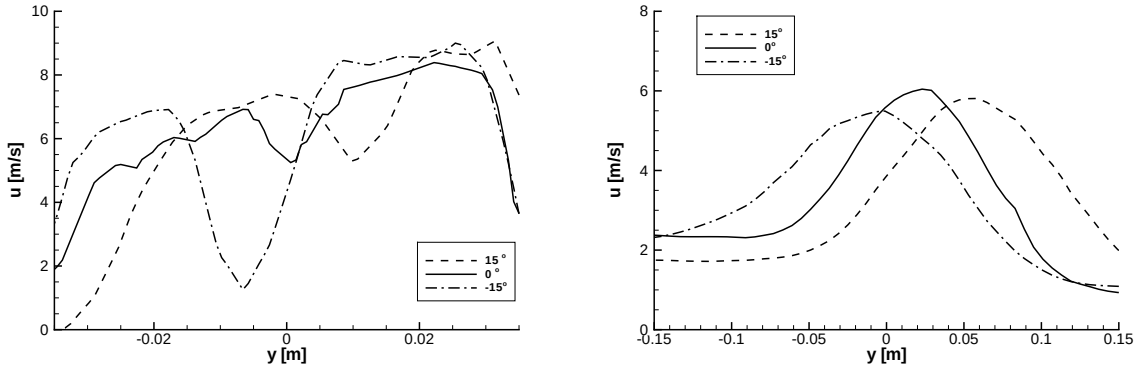

(a) $Plane\_1$ ($x = 10\ mm$) (b) $Plane\_2$ ($x = 500\ mm$)

Figure 11: One blade. Streamwise velocity prediction when its angle is changed.

sion in the velocity profile is produced by the blade near its trailing edge at the centre of the discharge nozzle. When an angle of -15^o is imposed, this minimum is more marked and a near wake behind the blade is observed. As consequence of this minimum, shear stress is increased and probably turbulence production. Furthermore, for both 15^o and -15^o, the outer peak ($y \geq 15mm$) is even increased. Moreover, reviewing predicted streamwise velocity profiles at $Plane\_2$ ($x = 500\ mm$), plotted in Figure 11(b), it can be seen that even though the blade angle is set to 15^o, air curtain discharge jet does not follow blade angle. A similar behaviour was observed experimentally. Furthermore, the jet is almost vertical when the angle is set to -15^o (right side,i.e. protected room).

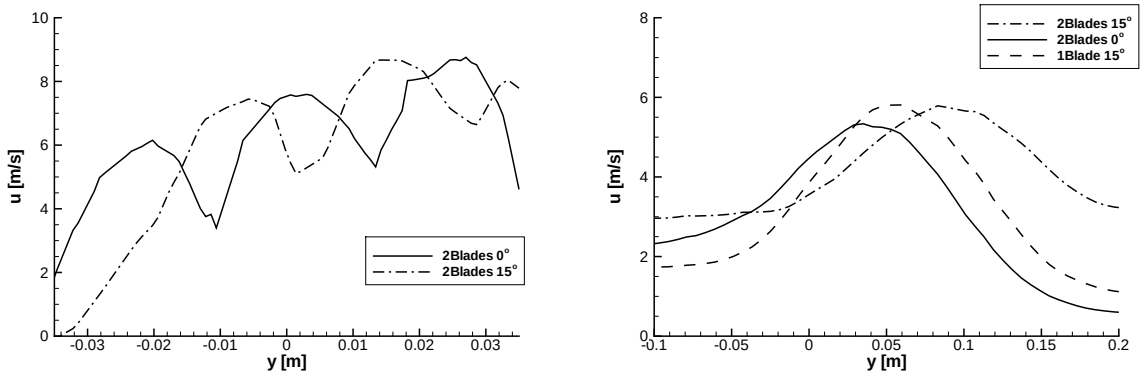

(a) $Plane\_1$ ($x = 10\ mm$) (b) $Plane\_2$ ($x = 500\ mm$)

Figure 12: Two blades. Streamwise velocity prediction when their angle is varied.

If two blades are used, two velocity minimums arise near discharge nozzle behind trailind edge of the blades, which disappear downstream forming a single jet (see Figure 12). If blades are vertical (discharge angle 0^o) three peaks are observed, and the jet is also slightly oriented towards the external left side (positive $y-$direction). Furthermore, when an angle of 15^o is set, the peak near external wall tends to vanish (see Figure 12(a)).

In Figure 12(b), predictions for one blade is depicted using dashed line for comparison purposes. As it can be seen in this Figure, by using two blades the flow is oriented better. However, its spreading rate is bigger, and air entrainment near jet borders is increased.

6 CONCLUSIONS

A set of experiments has been carried out in order to determine the actual fluid-flow characteristics of an air curtain prototype. Measurements have been done at the exit of the internal fans (plenum inlet), at the discharge of the air curtain prototype (discharge nozzle), and at some distance downstream. Experiments have revealed that velocity in the air curtain discharge nozzle presents numerous irregularities, and the turbulence intensity is relatively high.

The current group, plenum geometry plus blade for flow orientation, produce a jet with a skewed parabolic velocity profile with the peak shifted towards the left (external) side. Therefore, changes in the geometry of the plenum and/or blade shape should be introduced in order to have a similar profile to the desired one.

Influence of turbulence model, boundary conditions and computational domain has been numerically studied. At the inlet, superimposed fluctuations do not affect mean velocity near discharge nozzle, but inlet angle and the size of the computational domain downstram seems to play a more important role. Furthermore, the effect of using one or two blades has been analysed. It has been observed numerically and experimentally that one blade is not enough to control jet direction. The use of two blades improves flow orientation. However, further studies with another angles are still required.

ACKNOWLEDGEMENTS

This work has been financially supported by *Ministerio de Educacion y Ciencia*, Spain (Ref. PET2006-0343 and Ref. ENE2009-09496), and by a *Generalitat de Catalunya* Beatriu de Pinós postdoctoral fellowship (Ref. 2008 BP-A 00227).

REFERENCES

[1] H. B. Awbi. *Ventilation of Buildings*. Spon Press, 2003.

[2] G. Hetsroni, C. W. Hall, and A. M. Dhanak. Heat Transfer Properties of an Air Curtain. *ASAE Transactions*, 1:328–334, 1963.

[3] F. C. Hayes and W. F. Stoecker. Design Data for Air Curtains. *ASHRAE Transactions*, 2121:168–179, 1969.

[4] R. H. Howell and M. Shiabata. Optimum Heat Transfer Through Turbulent Recirculated Plane Air Curtains. *ASHRAE Transactions*, 86(1):188–200, 1980.

[5] R. Faramarzi and K. Kemp. Comparing Older and Newer Refrigerated Display Cases. *ASHRAE Journal*, Aug.:45–49, 1999.

[6] L. Guyonnaud, C. Solliec, M. Dufresne de Virel, and C. Rey. Design of air curtains used for area confinement in tunnels. *Experiments in Fluids*, 28:377–384, 2000.

[7] M. Havet, O. Rouaud, and C. Solliec. Experimental Investigations of an Air Curtain device Subjected to External Perturbations. *International Journal of Heat and Fluid Flow*, 24:928–930, 2003.

[8] Y. G. Chen and X. L. Yuan. Simulation of a cavity insulated by a vertical single band cold air curtain. *Energy Conversion Management*, 46:1745–1756, 2005.

[9] J. Partyka. Analitycal Design of an Air Curtain. *Int. Journal of Modelling and Simulation*, 15(1):14–22, 1995.

[10] K. Sirén. Technical Dimensioning of a Vertically Upwards Blowing Air Curtain. Part I. *Energy and Buildings*, 35:681–695, 2003.

[11] D. Stribling, S.A. Tassou, and D. Marriott. A Two Dimensional CFD Model of a Refrigerated Display Case. *ASHRAE Transactions*, 103(1):88–94, 1999.

[12] Y.T. Ge and S.A. Tassou. Simulation of the Performance of Single Jet Air Curtains for Vertical Refrigerated Display Cabinets. *Applied Thermal Engineering*, 21:201–219, 2001.

[13] H. K. Navaz, D. Dabiri, M. Amin, and R. Faramarzi. Past, Present, and Future Research Toward Air Curtain Performance Optimization. *ASHRAE Transactions*, 111:1083–1088, 2005.

[14] J. Cui and S. Wang. Application of CFD in evaluation and energy-efficient design of air curtains for horizontal refrigerated display cases. *International Journal of Thermal Sciences*, 43:993–1002, 2004.

[15] H.K. Navaz, R. Faramarzi, M. Gharib, D. Dabiri, and D. Modarress. The Application of Advanced Methods in Analyzing the Performance ot the Air Curtain in a Refrigerated Display Case. *Journal of Fluids Engineering*, 124(1):756–764, 2002.

[16] A. M. Foster, R. Barrett, S. J. James, and M. J. Swain. Measurement and prediction of air movement through doorways in refrigerated rooms. *International Journal of Refrigeration*, 25(8):1102–1109, 2002.

[17] J. J. Costa, L. A. Oliveira, and M. C. G. Silva. Energy savings by aerodynamic sealing with a downward-blowing plane air curtain-A numerical approach. *Energy and Buildings*, 38:1182–1193, 2006.

[18] A. M. Foster, M. J. Swain, R. Barrett, P. D'Agaro, and S. J. James. Effectiveness and optimum jet velocity for a plane jet air curtain used to restrict cold room infiltration. *International Journal of Refrigeration*, 29(5):692–699, 2006.

[19] A. M. Foster, M. J. Swain, R. Barrett, P. DAgaro, L. Ketteringham, and S. J. James. Three-Dimensional Effects of an Air Curtain Used to Restrict Cold Room Infiltration. *Applied Mathematical Modelling*, 31(6):1109–1123, 2007.

[20] J. E. Jaramillo, C. D. Pérez-Segarra, A. Oliva, and C. Oliet. Analysis of the Dynamic Behaviour of Refrigerated Space Using Air Curtains. *Numerical Heat Transfer, Part A*, 55(6):553–573, 2009.

[21] H. K. Navaz, M. Amin, S. C. Rasipuram, and R. Faramarzi. Jet entrainment minimization in an air curtain of open refrigerated display case. *International Journal for Numerical Methods for Heat and Fluid Flow*, 16(4):417–430, 2006.

[22] S.B. Pope. *Turbulent Flows*. Cambridge University Press, 2000.

[23] P. R. Spalart, S. Deck, M. L. Shur, K. D. Squires, M. K. Strelets, and A. Travin. A New Version of Detached-Eddy Simulation, Resistant to Ambiguous Grid Densities. *Theoretical and Computational Fluid Dynamics*, 20(2):181–195, 2006.

[24] O. Lehmkuhl, C. D. Perez-Segarra, R. Borrell, M. Soria, and A. Oliva. TERMOFLUIDS: A new Parallel unstructured CFD code for the simulation of turbulent industrial problems on low cost PC Cluster. In *Proceedings of the Parallel CFD 2007 Conference*, pages 1–8, 2007.

[25] R. W. Verstappen and R. M. Van Der Velde. Symmetry-preserving discretization of heat transfer in a complex turbulent flow. *Journal of Engineering Mathematics*, 54(4):299–318, 2006.

[26] H. H. Bruun. *Hot Wire Anemometry: Principles and Signal Analysis*. Oxford University Press, 1995.

[27] F.X. Trias, M. Soria, C.D. Pérez-Segarra, and A. Oliva. A Direct Schur-Fourier Decomposition for the Efficient Solution of High-Order Poisson Equations on Loosely Coupled Parallel Computers. *Numerical Linear Algebra with Applications*, 13(4):303–326, 2006.

[28] M. Germano, U. Piomelli, P. Moin, and W. H. Cabot. A Dynamic Subgrid-Scale Eddy Viscosity Model. *Physics of Fluids*, 3(7):1760–1765, 1991.

[29] D. K. Lilly. A Proposed Modification of the Germano Subgrid-Scale Closure Method. *Physics of Fluids*, 4(3):633–635, 1992.

[30] K. Mahesh, G. Constantinescu, and P. Moin. A Numerical Method for Large-Eddy Simulation in Complex Geometries. *Journal of Computational Physics*, 197:215–240, 2004.

[31] D. J. Glaze and S. H. Frankel. Stochastic Inlet Conditions for Large-Eddy Simulation of a Fully Turbulent Jet. *AIAA Journal*, 41(6):1064–1073, 2003.